

Control of Movement Variability and the Regulation of Limb Impedance

Daniel R. Lametti,¹ Guillaume Houle,¹ and David J. Ostry^{1,2}

¹Department of Psychology, McGill University, Montreal, Quebec, Canada; and ²Haskins Laboratories, New Haven, Connecticut

Submitted 28 August 2007; accepted in final form 29 September 2007

Lametti DR, Houle G, Ostry DJ. Control of movement variability and the regulation of limb impedance. *J Neurophysiol* 98: 3516–3524, 2007. First published October 3, 2007; doi:10.1152/jn.00970.2007. Humans routinely make movements to targets that have different accuracy requirements in different directions. Examples extend from everyday occurrences such as grasping the handle of a coffee cup to the more refined instance of a surgeon positioning a scalpel. The attainment of accuracy in situations such as these might be related to the nervous system's capacity to regulate the limb's resistance to displacement, or impedance. To test this idea, subjects made movements from random starting locations to targets that had shape-dependent accuracy requirements. We used a robotic device to assess both limb impedance and patterns of movement variability just as the subject reached the target. We show that impedance increases in directions where required accuracy is high. Independent of target shape, patterns of limb stiffness are seen to predict spatial patterns of movement variability. The nervous system is thus seen to modulate limb impedance in entirely predictable environments to aid in the attainment of reaching accuracy.

INTRODUCTION

The problem with making movements accurately is that it is very difficult to make exactly the same movement twice. In fact, movements are so inherently variable that professional basketball players spend much of their careers repeatedly practicing the movement of a successful free throw to make it as consistent and reproducible as possible. In the field of motor control, it has been proposed that movements are not perfect because of noise in neuromuscular signals (Harris and Wolpert 1998; van Beers et al. 2004). Recent neurophysiological evidence supports this idea and suggests that much of the noise in motor commands enters the signal in frontal lobe motor areas during the planning stages of movement (Churchland et al. 2006). Indeed, both behavioral and neurophysiological data seem to indicate that variability in movement is an inherent property of the motor system (Churchland et al. 2006; Fitts 1954; Harris and Wolpert 1998; van Beers et al. 2004). This being the case, a central problem in the field has been to elucidate a means by which the nervous system achieves accuracy in the face of movement variability. Here, we provide empirical evidence for a potential means of control that may act, independent of the motor commands that result in limb movement, to constrain movement variability. In a task involving highly varied movements we demonstrate that the spatial distribution of movement variability is related to limb impedance—the limb's resistance to displacement—and that when impedance is altered the nervous system predictably alters patterns of movement variability.

Address for reprint requests and other correspondence: D. J. Ostry, Department of Psychology, McGill University, 1205 Dr. Penfield Ave., Montreal, QC, Canada H3A 1B1 (E-mail: ostry@motion.psych.mcgill.ca).

Recently a substantial amount of research has examined potential control strategies that the nervous system might use to move accurately under conditions of noisy motor commands (Harris and Wolpert 1998; Haruno and Wolpert 2005; Todorov and Jordan 2002; van Beers et al. 2004). A control strategy that has been largely overlooked as a means to constrain movement variability in entirely predictable environments has been the nervous system's capacity to regulate limb impedance (Hogan 1985). Previous research has demonstrated that distinct from the commands that drive the limb, the nervous system can alter the limb's mechanical impedance through the simultaneous activation of antagonist muscle groups (Burdet et al. 2001; Feldman 1980; Franklin et al. 2007; Hogan 1985). Furthermore, behavioral work suggests that when movements are required to be more accurate, levels of muscle cocontraction and limb impedance tend to increase (Gribble et al. 2002; Selen et al. 2005). In other studies, where impedance was increased to counteract an environmental instability, a decrease in movement variability was observed in the direction of the impedance change even when the environmental instability was removed (Burdet et al. 2001). This evidence suggests that there may be a distinct relationship between the regulation of limb impedance and the regulation of movement variability.

In the present study, we have tested the idea that patterns of limb impedance predict spatial patterns of movement variability. To do this, we had subjects make movements from random starting locations about a circle into a target with shape-dependent accuracy requirements. We used a robotic device to assess the static component of limb impedance (stiffness) and to measure patterns of movement variability as the subject reached the target. Our hypothesis was that in a situation involving widely varying movements the nervous system would utilize the control of limb stiffness to aid in the attainment of accuracy. Indeed, we show that stiffness increases in directions where required accuracy is high and that movement variability in these same directions is reduced. Moreover, we demonstrate that independent of target shape and in environments that are always predictable, the spatial distribution of movement endpoints is significantly related to patterns of limb stiffness. The findings suggest that the nervous system may use the regulation of limb impedance more broadly than previously thought as a means to regulate variability in movement.

METHODS

Subjects

In all, 24 young adults (13 females) between the ages of 18 and 30 took part in the experiment. The experiment was approved by the

The costs of publication of this article were defrayed in part by the payment of page charges. The article must therefore be hereby marked "advertisement" in accordance with 18 U.S.C. Section 1734 solely to indicate this fact.

McGill University Ethics Board. All subjects were right-handed and had normal or corrected-to-normal vision.

Apparatus

Subjects grasped the handle of a two-joint robotic arm (Interactive Motion Technologies, Cambridge, MA) and were positioned such that the angle at the elbow was 90° and the angle at the shoulder was 45° relative to the frontal plane. Shoulder movement was restricted by a harness. Movements were made in the horizontal plane and the subject's arm was supported by an air-sled to reduce friction. A six-axis force torque transducer (ATI Industrial Automation, Apex, NC) was mounted above the handle of the manipulandum such that forces applied by the subject could be measured. Optical encoders (16-bit; Gurley Precision Instruments, Troy, NY) sensed joint angles. Movements of the robot handle in the horizontal plane were mirrored by a cursor on a monitor placed at eye level in the frontal plane. The data were sampled at 400 Hz.

Experimental task

Subjects made movements to one of four targets (see Fig. 1). One of the targets was a circle and the other three targets were elliptical in shape. A vertical target had a major axis at 90° , a horizontal target had a major axis at 0° , and a diagonal target had a major axis at 135° (as measured counterclockwise from the horizontal). The area of each target was $4\pi \text{ cm}^2$. Six different subjects were tested for each target shape. The manipulation had three parts that were carried out in a single session. The same target was used for each of these three parts. In phase one, subjects were required to position the hand within the displayed target and hand stiffness was measured under stationary conditions (see *Stiffness estimation*). In phases two and three subjects were required to make movements into the target from random starting positions about a circle (12.5 cm radius) centered on the target (see Fig. 2A). Phase two consisted of 150 training trials. This phase enabled subjects to learn the transformation between the robotic arm in the horizontal plane and the cursor displayed in the vertical plane and also allowed kinematic variability to stabilize. Phase three involved an average of 252 trials (the exact number of trials was dependent on subject accuracy) and also included trials in which limb stiffness was measured at the end of movement (see Fig. 2B and *Stiffness estimation*). On each trial, when signaled to move, subjects had to leave the start position and enter the target within 400 ms. Subjects were instructed to come to a complete stop within the boundaries of the target. For movements in which the subject entered the target in $<400 \text{ ms}$ and stopped accurately within the boundaries of the target, the target turned blue and subjects were awarded points on a score counter in the top left corner of the monitor. For movements in which the subject failed to enter the target within 400 ms or left the target without completely stopping within its boundaries, the target turned green and points were removed. After feedback was given on the accuracy of the movement, the robotic arm brought the subject's hand (by servo-control) to the next random starting location. The task was then repeated.

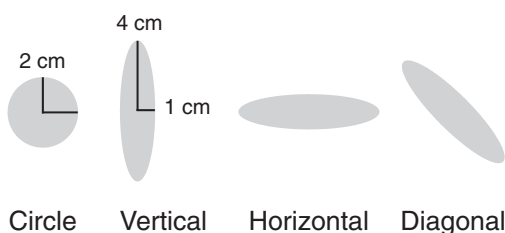


FIG. 1. Target shapes. Subjects had to move to one of 4 targets that differed in their directional accuracy requirements. Area of all 4 targets was the same.

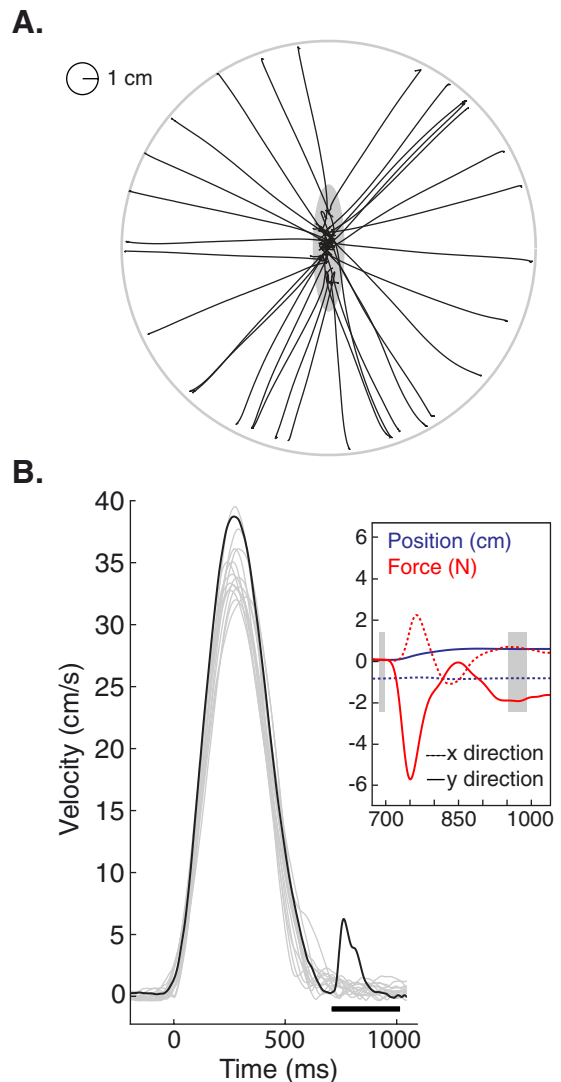


FIG. 2. Movement paths, velocity, and force profiles. A: 32 typical hand paths are shown for a representative subject during the stiffness measurement phase of the experiment. Subjects made movements from random starting points about a circle of radius 12.5 cm into a target. In this case, subjects moved into a vertical target. Each of the movements shown here was followed by a displacement for purposes of stiffness measurement. B: tangential velocity profiles are shown for typical movements made during the experiment. At the end of the movement shown with a black velocity profile, a perturbation was delivered for purposes of stiffness measurement. Period of the perturbation is shown with a black horizontal line. Inset box: restoring force in the x and y directions (blue traces) and position in the x and y directions (red traces) during the perturbation. Shaded regions represent the intervals from which restoring force and position were sampled to estimate limb stiffness.

Analysis of kinematic variability

Position and force were low-pass filtered at 30 Hz. Hand position was numerically differentiated to estimate velocity. Movement start and end were scored at 5% of peak tangential velocity. Trials in which the tangential velocity profile showed multiple peaks were excluded. Trials were also excluded if the movement endpoint fell outside a 99% confidence interval encompassing all end positions from that phase of the experiment. In total about 7% of trials were rejected based on these criteria. We felt that this rejection rate was acceptable because the task involved random starting locations rather than well-practiced movements in a small set of directions.

To examine kinematic variability at the end of movement, covariance matrices were calculated from the acceptable movement end-

points. Using the covariance matrix, the distributions of endpoints were displayed as 95% confidence ellipses. Singular-value decomposition was used to compute the orientation and size of each ellipse (Shiller et al. 2002; van Beers et al. 2004). To assess changes in kinematic variability over time, movement endpoint positions were binned into groups of 15 consecutive movements and the area of 95% percent confidence ellipses encompassing the observations in each bin was found. For each target shape, the mean variability at the start of training, at the start of stiffness measurement, and just before the end of the experiment were compared using ANOVA (mixed-factor ANOVA with Bonferroni-corrected pairwise comparisons).

Stiffness estimation

Stiffness was estimated using a standard method (Burdet et al. 2001; Darainy et al. 2004, 2006, 2007; Gomi and Kawato 1997; Gomi and Osu 1998; Mussa-Ivaldi et al. 1985) in which the limb is displaced under position servo-control and restoring force is measured. The relationship between change in force and change in position of the limb due to the perturbation can be written as

$$dF = KdP \quad (1)$$

or, in matrix notation

$$\begin{bmatrix} dF_x \\ dF_y \end{bmatrix} = \begin{bmatrix} K_{xx} & K_{xy} \\ K_{yx} & K_{yy} \end{bmatrix} \begin{bmatrix} dP_x \\ dP_y \end{bmatrix} \quad (2)$$

In Eqs. 1 and 2, dF is the change in force, dP is the change in position, and K represents stiffness at the hand in two dimensions. K_{xx} gives the resistive force of the limb in x per unit displacement in x , K_{xy} is the force in x per unit displacement in y , and so forth.

In the present study, the limb was perturbed by a 0.55-cm (SD 0.01 cm) servo-controlled displacement of the robot's handle. The displacement was built up over 75 ms, held for 250 ms, and then released (see *inset* in Fig. 2B). To estimate K , perturbations were delivered in multiple directions. For each subject four perturbations were delivered in each of eight directions (0, 45, 90, 135, 180, 225, 270, and 315°) in random order (32 in total). Differences in the mean value of hand position between a 10-ms window immediately before the perturbation and a 30-ms window starting 250 ms after the start of the servo-displacement (175 ms after the start of the hold phase) gave values for dP_x and dP_y (see *inset* in Fig. 2B, shaded regions). Differences in the mean values of force found during the same windows gave values for dF_x and dF_y (32 of each). Linear regression was then used to estimate K .

Displacements were delivered for purposes of stiffness estimation during phase one and phase three of the experiment. Displacements were applied only when the hand was stationary—in the target zone with a tangential velocity of <4 mm/s. In phase one, subjects rested within the target and displacements were delivered at random every 8 to 12 s. In phase three, displacements were delivered at the end of some movements in which subjects satisfied movement timing and accuracy requirements (see *Experimental task*). On average one good movement in three received a perturbation (order randomized). Because only a subset of movements met the timing and accuracy requirements of the task the average subject received only one displacement every seven movements. Subjects were instructed to ignore any felt displacements.

To ensure that the limb was stationary during stiffness measurement, measures of dP and corresponding measures of dF were not included if at any point during the servo-displacement measurement window the tangential velocity of the hand reached 4 mm/s. Based on this criterion the average subject had 3 of 32 measurements eliminated. To assess the possibility of voluntary subject intervention we examined the variability in measured restoring force during the hold phase of the perturbation. Our assumption was that voluntary intervention would be reflected by significant variation in restoring force

due to the subject's response. The average SD in the restoring force during the measurement window was found to be 0.07 N. Indeed, the average SD in restoring force from 200 to 300 ms after the start of the perturbation was only 0.13 N. There was thus little evidence of intervention on the part of the subject during stiffness measurement.

Although subjects could have received a displacement for purposes of stiffness estimation at any position within a target, on average for the elliptical targets, the displacement actually occurred within ± 1.55 cm (SD 0.48 cm) of the origin along the major axis of the target and ± 0.45 cm (SD 0.03 cm) of the origin on the minor axis. On average for the circular target, the displacement occurred within ± 1.15 cm (SD 0.15 cm) of the origin along the x -axis of the target and ± 0.95 cm (SD 0.17 cm) of the origin on the y -axis. It was previously shown that the orientation of the major axis of the stiffness ellipse rotates by about 1° per centimeter change in limb position (calculated from Table 6 in Mussa-Ivaldi et al. 1985). Mussa-Ivaldi et al. also showed that changes in ellipse orientation are mirrored along a right-left axis from the midline and along a proximal-distal axis from the body. That is, as hand position moves to the right of the midline the orientation of the stiffness ellipse rotates to the right and as hand position moves to the left of the midline the orientation of the stiffness ellipse rotates to the left. A similar effect is seen as hand position moves proximal to the body or distal to the body. In the present experiment, the limb positions at which measurements of stiffness were taken differed randomly by a very small amount around the center of each target. Based on the work mentioned earlier, it can be reasonably assumed that on individual trials, contributions to measures of stiffness due to changes in limb position are small and, that over several trials, these contributions are likely to have canceled each other out.

Analysis of stiffness data

Limb stiffness was visualized as an ellipse, where the major axis is the direction of maximum stiffness and the minor axis is the direction of minimum stiffness. Singular value decomposition was used to determine the size and orientation of the ellipse (Gomi and Osu 1998; Mussa-Ivaldi et al. 1985).

The degree to which the stiffness ellipse adequately represents the limb's restoring force in response to an external perturbation was determined by finding the correlation between the actual restoring force and the restoring force as predicted by the stiffness matrix. To do this, predicted restoring force was determined by taking the product of the stiffness matrix and the vector of actual hand displacements. The predicted restoring force was then averaged over all cases in each perturbation direction and correlated with the actual restoring force also averaged over instances in each perturbation direction (Franklin et al. 2007). Over the four targets, the percentage of variance in the actual restoring force accounted for by the stiffness matrix ranged from 76 to 98% for stiffness as measured at the end of movement, and 94 to 96% for stiffness as measured at rest. Thus the computed stiffness ellipses provided a good representation of the restoring force produced by the limb in response to a perturbation.

The extent to which stiffness changed for movements to different targets was evaluated by comparing stiffness ellipse orientations for the different targets and by assessing the extent of stiffness change relative to measures obtained for the same target when the limb was stationary. For the latter, stiffness measures were obtained in relation to the directional accuracy requirements of each of the four targets (see Fig. 1). For each of the three elliptical targets, the direction of greatest required accuracy was perpendicular to the major axis of the target (see Fig. 4A, black arrows) and the direction of least required accuracy was parallel to the major axis. The corresponding values of stiffness in the directions of greatest and least accuracy were the magnitudes of stiffness in these two directions. For each elliptical target, resting stiffness in the direction of greatest required accuracy was compared with stiffness at the end of movement in this same

direction. The same comparison was made for stiffness in the direction of least required accuracy. For the circular target the vector magnitudes of resting stiffness along the x -axis and y -axis were compared with the same measures of stiffness at the end of movement. Comparisons were done across all conditions using ANOVA (mixed-factor ANOVA, with Bonferroni-corrected pairwise comparisons).

Correlation between stiffness and kinematic variability

To examine the relationship between stiffness and kinematic variability, stiffness ellipses measured at the end of movement were compared with endpoint variability ellipses that were constructed from all endpoints from phase three of the experiment. For each subject, measures of stiffness and variability were obtained in the direction of the major axis of the stiffness ellipse. In the case of stiffness, the measure was simply twice the magnitude of the maximum eigenvalue. In the case of variability, the measure was the length of a straight-line path spanning the variability ellipse in the direction of maximum stiffness. Measures of stiffness and variability were also obtained in the direction of the minor axis of the stiffness ellipse. Through use of these data, the dependence of kinematic variability on stiffness was assessed using linear regression.

Stiffness dependence on the direction of the preceding movement

To assess the extent to which the control of stiffness was independent of the motor commands that move the limb, the dependence of measured stiffness on the direction of the preceding movement was examined in two ways. First, the dependence of the direction of the measured restoring force on the direction of the preceding movement was examined using circular-circular correlation (Fisher 1993). Next, the dependence of the magnitude of the restoring force on the direction of the preceding movement was evaluated for each target

shape. We also evaluated the relationship between restoring force magnitude and the angle between the preceding movement and the direction of displacement. In both cases, a nonlinear regression was performed based on a sinusoidal function. The sinusoid took the form

$$F = b_1 \sin x + b_2 \cos x + b_3 \quad (3)$$

where F is the restoring force magnitude, x is the direction of preceding movement or the difference between the direction of preceding movement and the displacement direction, b_1 and b_2 together specify phase and amplitude, and b_3 is the mean of the data. The best fit is thus modeled as a sinusoidal relationship in which both magnitude and phase can vary.

RESULTS

The experiment had three parts in which subjects moved the handle of a robotic arm to targets of different shape. In phase one, limb stiffness was estimated by using servo-controlled displacements of the arm and simultaneous recording of the limb's resistive force (restoring force) while subjects rested within a target. In phase two, the training phase, subjects moved the robot handle from random starting locations about a circle into the same target. In phase three, the stiffness measurement phase, subjects made similar movements of the handle into the same target and servo displacements identical to those in phase one were delivered just after the end of movement to estimate limb stiffness.

Figure 3A shows patterns of variability of hand position at the end of movement (95% confidence ellipses) for individual subjects at the start of the training phase (blue ellipses) and 150 trials later at the start of the measurement phase (red ellipses).

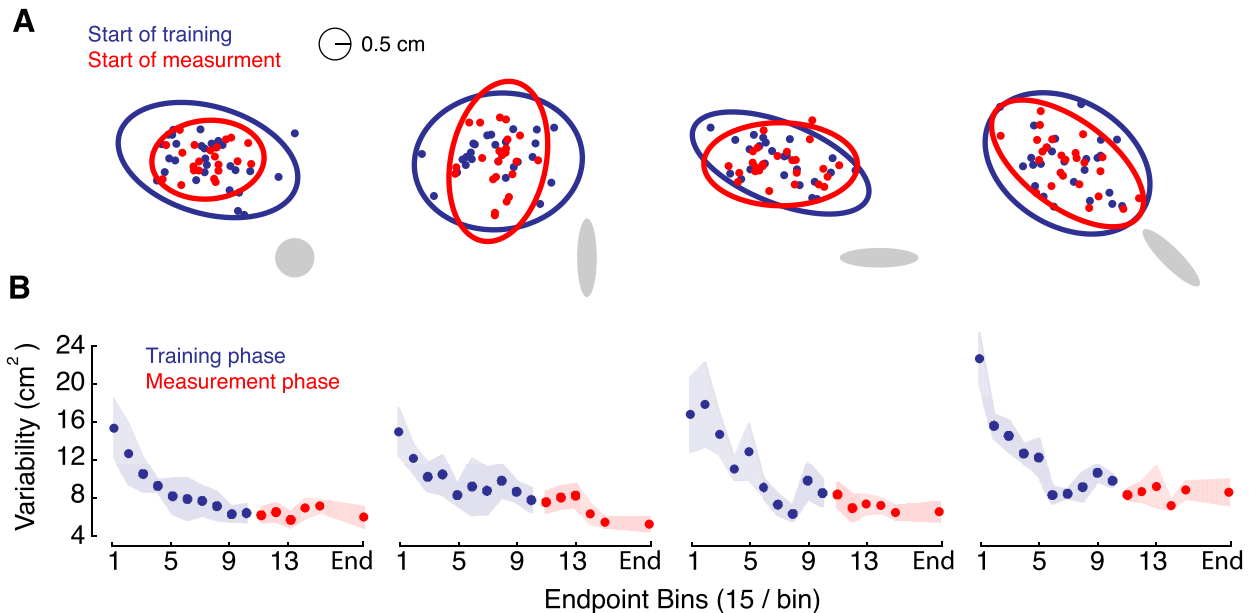


FIG. 3. Kinematic variability decreases with training and remains constant during stiffness measurement. *A*: endpoints of movement taken from representative subjects (one subject for each of the 4 target shapes). 95% confidence ellipses are based on the 25 endpoints of the same color. Blue ellipses represent the distribution of endpoints for the first 25 movements in the experiment; red ellipses show the distribution of endpoints for the first 25 movements at the start of the stiffness measurement phase. Variability is seen to approximate target shape. Targets are shown in gray. *B*: observed changes in kinematic variability are shown over the course of training. Area of 95% confidence ellipses constructed from consecutive bins of 15 endpoints is averaged across subjects. Shaded regions represent ± 1 SE. Ten blue points give average endpoint variability over the first 150 (training) trials in the experiment. Next 5 red points represent average endpoint variability for the first 75 movements in the stiffness measurement phase of the experiment. Last red point (End) gives average variability for the last 15 movements in the experiment. It can be seen that endpoint variability decreased over the training phase of the experiment. During stiffness measurement, variability remained consistent and was not different across target shapes.

At the start of the training phase endpoint variability is high; over the course of training, the distribution of movement endpoints decreases in size to approximately half the area of the target. In the case of the elliptical targets the distribution of movement endpoints came to approximate the shape of the targets.

To track changes in variability with training, the area of 95% confidence ellipses, based on bins of 15 consecutive movement endpoints, were averaged across subjects that moved to the same target (Fig. 3B). For each target shape, a reliable decrease in endpoint variability [$F_{(2,38)} = 51.95$, $P < 0.001$] was observed over the course of training. For these same targets, endpoint variability at the start of stiffness measurement was not different from endpoint variability at the end of the experiment ($P > 0.05$). Moreover, over both the training phase and stiffness measurement phase, endpoint variability was not different across target shapes [$F_{(6,38)} = 0.58$, $P > 0.05$]. These results suggest that by the end of training all subjects had learned to make equally accurate movements and this level of movement accuracy did not change during stiffness measurement.

Limb stiffness is modulated in relation to the accuracy requirements of targets

Limb stiffness was visualized as an ellipse, in which the major axis is the direction of maximum stiffness and the minor axis is the direction of minimum stiffness (Burdet et al. 2001; Darian et al. 2004; Gomi and Osu 1998; Mussa-Ivaldi et al.

1985). Figure 4A shows stiffness ellipses averaged over subjects following movements to different targets (red ellipses) and averaged ellipses obtained under stationary conditions within the same targets (blue ellipses). It can be seen that for the targets with directional accuracy requirements, patterns of limb stiffness at the end of movement were different in shape and orientation compared with patterns of static (resting) stiffness observed within the same targets before training. For subjects that moved to the circular target, stiffness at the end of movement was not substantially different from stiffness in statics.

Differences in stiffness ellipse orientation between the four target shapes and across the conditions of the experiment were assessed quantitatively (Fig. 4B). Under static conditions, we found no differences in ellipse orientation for the four targets ($P > 0.05$, for each comparison). Following movement, the ellipse orientations for the vertical, horizontal, and diagonal target conditions were each reliably different from one another ($P < 0.001$, in each case). The ellipse orientations for the vertical and diagonal target conditions also differed from that of the circle condition ($P < 0.001$, in both cases). Moreover, we observed reliable changes in the orientation of the major axis of the stiffness ellipse in each of the vertical, horizontal, and diagonal target conditions relative to stiffness measured at rest ($P < 0.001$, $P < 0.05$, $P < 0.001$, respectively). For subjects that moved to each of these targets the major axis of the stiffness ellipse was seen to assume an orientation that was more orthogonal to the major axis of the target. For the circular target, the orientation of the major axis of stiffness as measured

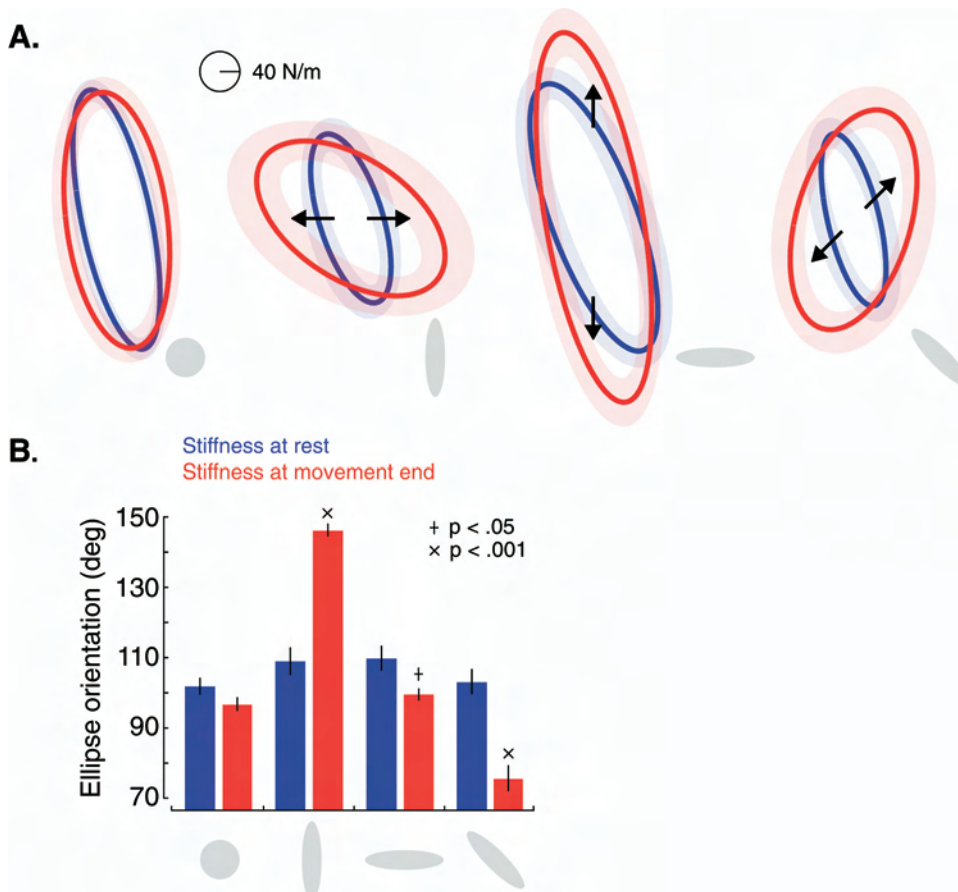


FIG. 4. Patterns of limb stiffness vary with target shape. *A*: average stiffness ellipses for each target shape (targets are shown in gray). Blue ellipses show stiffness measured with the hand at rest in the target before training; red ellipses represent stiffness as measured just after the end of movement to the same target. Shaded regions represent ± 1 SE in stiffness. Black arrows represent directions of greatest required target accuracy. In these directions stiffness at the end of movement was seen to significantly increase ($P < 0.001$) compared with that at rest. *B*: mean orientation of the major axis of the stiffness ellipse for each target shape. At the end of movement, the orientation of the stiffness ellipse varies in a systematic fashion with target shape, whereas stiffness ellipse orientation as measured at rest is similar across target shapes.

at the end of movement was not different from the orientation as measured at rest ($P > 0.05$).

An examination of Fig. 4A shows that after training to the elliptical targets stiffness was seen to increase in directions where required target accuracy is high (arrows). To quantify differences in stiffness between rest conditions and after movement, for the elliptical targets, the vector magnitudes of stiffness were obtained in directions of greatest required accuracy and in directions of least required accuracy. For the circular target, the vector magnitudes of stiffness were obtained in the directions of the x -axis and y -axis. For all three of the elliptical targets stiffness at the end of movement is seen to be greater in directions where required movement accuracy is high ($P < 0.001$ in each case; arrows in Fig. 4A show directions of reliable stiffness increase). For these same targets, no difference in stiffness is observed in directions where required movement accuracy is low ($P > 0.05$ in each case; directions perpendicular to arrows in Fig. 4A). For the circular target, which had no specific directional accuracy requirements, stiffness at the end of the movement in the directions of the x -axis and y -axis is the same as stiffness at rest in these same directions ($P > 0.05$ for both directions). This result suggests that for targets with specific directional accuracy requirements,

stiffness of the limb at the end of movement is altered to reflect the shape of the target.

Limb stiffness predicts kinematic variability

To examine the idea that there is a relationship between patterns of measured limb stiffness and patterns of observed movement variability, stiffness ellipses estimated at the end of some movements were compared with kinematic variability ellipses consisting of all endpoints from the same phase of the experiment. Figure 5A shows individual examples of variability and stiffness for the four targets (targets shown in gray). Superimposed error cones give the mean orientation (± 1 SE) of stiffness (red) and variability (blue) across subjects for each target shape. It can be seen that stiffness and kinematic variability are inversely related. This relationship is particularly striking in the case of the circular target where patterns of limb stiffness appear to be a better predictor of patterns of movement variability than the actual shape of the target. For this target, patterns of kinematic variability were not circular but were elliptical, with a major axis that was roughly perpendicular to the major axis of the stiffness ellipse ($75.2 \pm 7.6^\circ$ SD, difference in orientation).

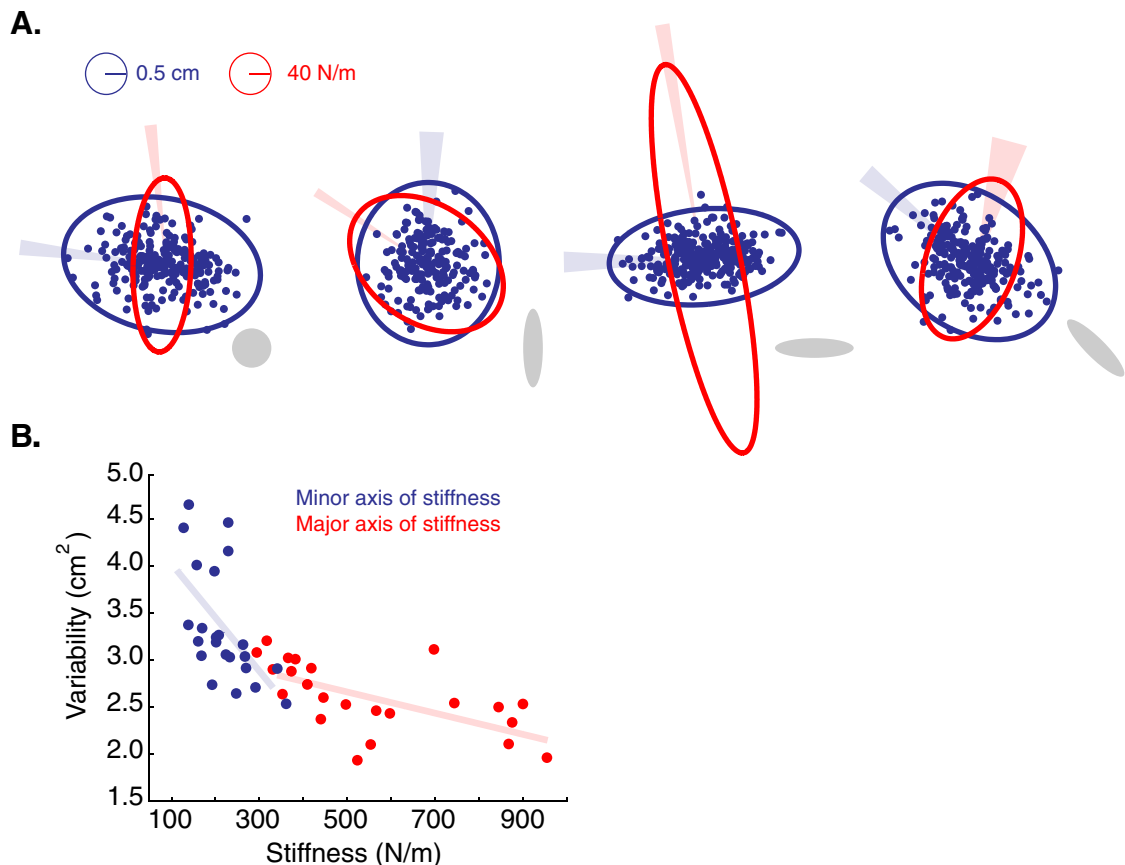


FIG. 5. Patterns of limb stiffness are related to spatial patterns of kinematic variability. *A*: relationship between stiffness and kinematic variability is shown for 4 representative subjects. Targets are shown in gray. Blue ellipses are 95% confidence ellipses constructed from all endpoints from the stiffness measurement phase of the experiment; superimposed red ellipses show stiffness at the end of movement for the same subject. Blue and red cones show the mean orientation ± 1 SE of kinematic variability and stiffness averaged over all subjects for a given target. It can be seen that stiffness and kinematic variability are roughly orthogonal. Stiffness is high in directions in which kinematic variability is low and vice versa. *B*: dependence of kinematic variability on stiffness is shown for the major and minor axes of the stiffness ellipse. Red dots show the magnitude of the major axis of the stiffness ellipse, measured at the end of movement plotted against variability in the same direction. Blue dots show the stiffness magnitude for the minor axis of the stiffness ellipse and corresponding variability measures. Solid lines are the lines of best fit as estimated by linear regression. It may be seen that there is an inverse relationship between stiffness and kinematic variability.

To quantify the relationship between stiffness at the end of movement and spatial patterns of movement variability we examined variability in directions in which stiffness was greatest and also in directions in which stiffness was least. Our rationale for doing this was based on the fact that the shape of the stiffness ellipse is defined by the magnitude of its major and minor axes. Specifically, a relationship between the magnitude of the major axis of stiffness and variability in that same direction, and a similar relationship between the magnitude of the minor axis of stiffness and variability in that direction, would indicate that, independent of target shape, patterns of limb stiffness predict spatial patterns of movement variability. Figure 5B shows the relationship between the major axis of stiffness and variability in the same direction (red) and the minor axis of stiffness and variability in the same direction (blue). In both cases, a significant negative correlation was observed between stiffness and kinematic variability ($r = -0.65$, $P < 0.001$ and $r = -0.56$, $P < 0.005$, respectively). In directions in which stiffness was high, variability was low and vice versa. These results suggest that patterns of limb stiffness predict spatial patterns of movement variability.

Stiffness change is independent of movement direction

In the present study, stiffness measurements were taken after movements from random directions and consistent target-based changes in limb stiffness were observed. This finding suggests that the nervous system can regulate limb impedance independent of the commands that move the limb. We quantitatively explored this idea by examining the extent to which the restoring force of the limb after servo-displacement might depend on the specifics of the preceding movement. We first assessed whether the vector direction of measured restoring force was best predicted by the direction of the preceding movement or the direction of the displacement used for stiffness measurement. We next examined the relationship between the magnitude of the restoring force and the preceding movement direction.

We used circular–circular correlation to examine the relationship between restoring force direction and both the direction of the preceding movement and the direction of limb displacement. The circular–circular correlation between limb displacement direction and restoring force direction was 0.81 ($P < 0.001$; see Fig. 6A). In contrast, the circular–circular correlation between the direction of the preceding movement and restoring force direction was 0.01 ($P > 0.05$). We next examined the dependence of the magnitude of restoring force on movement direction. If the preceding movement influenced restoring force, and movements were started from random positions about a circle, then one might expect a sinusoidal relationship between the direction of movement and the measured restoring force. To test this, we assessed the relationship between restoring force magnitude and the direction of the preceding movement using a sinusoidal function (see METHODS). On average, the sinusoid accounted for only 1.20% more of the variance in the data than the mean ($P > 0.05$, for each target). Another more likely possibility was that the magnitude of the restoring force might vary as a function of the angle between the displacement direction and the direction of the preceding movement. To test this, we again used the same sinusoidal

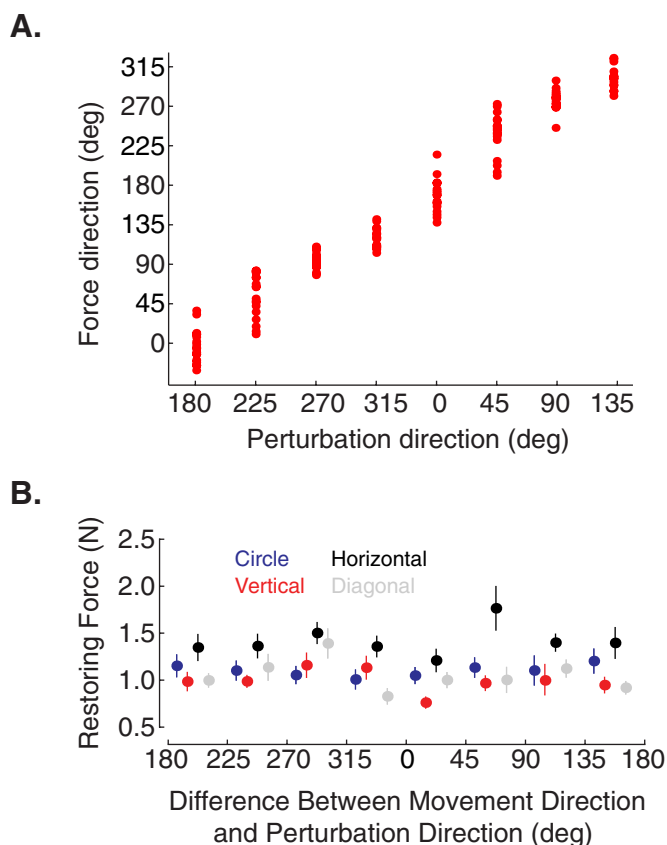


FIG. 6. Stiffness change is independent of movement direction. *A*: direction of restoring force is plotted over subjects against the direction of displacement used for stiffness measurement. Direction of restoring force is predicted by the direction of limb displacement. *B*: for each target restoring force magnitude is plotted against the difference between the direction of the preceding movement and the direction of the perturbation. Data for the circular, vertical, horizontal, and diagonal targets are represented by blue, red, black, and gray points, respectively. To analyze trends, restoring force was averaged within 45° bins. Error bars represent $\pm 1SE$. Measured restoring force can be seen to be independent of the angle between the preceding movement direction and the displacement direction.

function but this time we assessed the relationship between restoring force magnitude and the difference between the preceding movement direction and the displacement direction. Figure 6B plots this relationship for each target separately with the data binned based on 45° intervals. On average, the sinusoid accounted for 0.45% more of the variance than the mean ($P > 0.05$, for each target).

In combination, the analyses presented here demonstrate that both the direction and magnitude of restoring force depend quite weakly (if at all) on the direction of the preceding movement. This suggests that the target-based changes in limb stiffness observed were likely to have been centrally specified independent of the motor commands that resulted in the movement of the limb.

DISCUSSION

We have identified a means by which the nervous system can act to constrain movement variability and attain accuracy when reaching to targets. Previous research has shown that muscle coactivation and overall limb stiffness scale globally as a function of target size (Gribble et al. 2002; Selen et al.

2005). However, no direct measures of limb stiffness have been made in the context of movements with different precision requirements. Here we show that the nervous system can significantly modify the pattern of limb stiffness in relation to the shape of the target such that stiffness is increased in directions in which greatest accuracy is required. Stiffness changes are coupled to variation in movement kinematics in a manner consistent with the idea that stiffness control is used to regulate patterns of endpoint variability. Limb stiffness is seen to predict spatial patterns of movement variability such that in directions where stiffness is high variability is low and vice versa.

Limb stiffness modulation in statics and during movement

In the present study stiffness was measured just at the completion of movement. We chose this approach to measuring stiffness because our movements were made from random starting locations and the measurement of stiffness during movement requires highly repetitive movements (Burdet et al. 2001; Darainy et al. 2007; Franklin et al. 2004, 2007). However, because movement-related EMG activity persists for several hundred milliseconds after movement end (Gribble and Ostry 1998; Suzuki et al. 2001) it is presumably possible to assess changes in limb stiffness that occur before movement end by measuring stiffness just at the completion of movement. The range of stiffness modulation observed here is consistent with the idea that stiffness was modified before the end of movement but is not consistent with previous reports of stiffness modulation in statics. The range of stiffness modulation in the present study was about 70° . A recent study that examined adaptive changes in limb stiffness during movement found that subjects could similarly alter the direction of maximum limb stiffness by about 70° (Franklin et al. 2007). In contrast, studies that have examined stiffness regulation under purely static conditions have consistently found a range of stiffness modulation that is much less than this (Darainy et al. 2004, 2006; Gomi and Osu 1998; Mussa-Ivaldi et al. 1985; Perreault et al. 2002). For example, with the limb in a static position Perreault et al. (2002) gave subjects real-time visual feedback of their stiffness ellipse and instructed them to rotate it as much as possible in the clockwise or counterclockwise direction by cocontracting different muscle groups. Under these conditions, the range of stiffness regulation was about 20° . Other studies that have used different techniques to assess static stiffness regulation have obtained very similar estimates (Darainy et al. 2004, 2006; Gomi and Osu 1998). Thus the range of stiffness modulation in the present study is consistent with the idea that the patterns of stiffness measured here were likely modified before movement end.

If limb stiffness was altered before the end of movement it may seem paradoxical that no relationship was found between restoring force and the direction of the preceding movement. Yet, as studies involving the adaptation of limb stiffness to destabilizing loads have repeatedly demonstrated (Burdet et al. 2001; Franklin et al. 2004, 2007), during movement, the nervous system can precisely alter limb stiffness independent of the commands that move the limb. Our findings are entirely consistent with these results.

Limb stiffness control as an aid to the attainment of accuracy

The patterns of endpoint variability observed in the present study are consistent with the idea that limb stiffness was modulated before the end of movement to aid in the attainment of accuracy. Independent of target shape it was determined that, in directions of high limb stiffness, kinematic variability was low and in directions of low limb stiffness, kinematic variability was high. Such a relationship is in agreement with previous reports demonstrating that when stiffness was adapted to counteract an environmental instability movement variability was reduced in approximately the same direction as the stiffness increase, even when the instability was removed (Burdet et al. 2001). Unlike previous reports, this study provides a first demonstration of precise stiffness control in an environment that is consistently predictable.

Several prior studies have investigated patterns of endpoint variability during load-free reaching (Gordon et al. 1994; van Beers et al. 2004). In our study, variability at the start of training was high. This was presumably due in part to the use of air-sleds (van Beers et al. 2004) and in part because subjects had to learn the transformation between the robot and the visual display. By the end of training, the spatial extent of endpoint variability was similar to that observed in previous studies that had a similar movement extent and target size (Gordon et al. 1994). However, orientation of the endpoint variability ellipse here is different from that in previous studies. In both Gordon et al. (1994) and van Beers et al. (2004) it was observed that, when subjects reached toward a circular target from a single starting point, the major axis of the variability ellipse was oriented in the direction of movement. Here, for a similar circular target, the major axis of the variability ellipse had an orientation that was roughly perpendicular to the direction of maximum limb stiffness. The difference between previous reports and our results may lie in the tasks that were used. In both Gordon et al. (1994) and van Beers et al. (2004) subjects made highly practiced center-out movements to targets. In our study, subjects made movements from random starting locations about a circle into targets. By randomizing the starting point of movements it was hypothesized that impedance control might be favored to help achieve accuracy. That is, although the motor commands to move the limb had to be modified on a trial-to-trial basis to meet the requirements of the task, a cocontraction command related to achieving target accuracy could be essentially held constant. If such a control strategy were used, one would expect that even for a circular target, patterns of limb stiffness should predict patterns of kinematic variability and, that measures of restoring should be largely independent of the specifics of individual movements. Both results were observed.

It is important to note that our results only suggest that given the right circumstances stiffness control can be used to help regulate accuracy. Indeed, in other circumstances (Gordon et al. 1994; van Beers et al. 2004) stiffness control may be used to a lesser extent (if at all). Nonetheless, the task we used in this experiment resembles goal-directed movements that are frequently encountered in everyday life, that is, the targets we reach toward often remain fixed whereas the movement paths we take typically vary. Thus in predictable environments

impedance control might be used much more than previously thought as an aid to the attainment of reaching accuracy.

In summary, much of the work to date on impedance control has dealt with the problem of stabilizing movements in the context of unpredictable mechanical loads. The results presented here demonstrate that stiffness regulation applies broadly even in environments that are entirely predictable. Indeed, patterns of limb stiffness were seen to predict spatial patterns of movement variability. The CNS thus has the ability to precisely control limb impedance to constrain movement variability and aid in the achievement of reaching accuracy.

ACKNOWLEDGMENTS

We thank P. L. Gribble and J. R. Flanagan for helpful comments and A. A. Mattar, M. Darainy, P. Lauzon, S. M. Nasir, T. Ito, and Z. Shehzad for advice and support.

GRANTS

This research was supported by the National Institute of Child Health and Human Development Grant HD-48924. D. Lametti is supported by the Natural Sciences and Engineering Research Council of Canada and McGill University.

REFERENCES

- Burdet E, Osu R, Franklin DW, Milner TE, Kawato M.** The central nervous system stabilizes unstable dynamics by learning optimal impedance. *Nature* 414: 446–449, 2001.
- Churchland MM, Afshar A, Shenoy KV.** A central source of movement variability. *Neuron* 52: 1085–1096, 2006.
- Darainy M, Malfait N, Gribble PL, Towhidkhal F, Ostry DJ.** Learning to control arm stiffness under static conditions. *J Neurophysiol* 92: 3344–3350, 2004.
- Darainy M, Malfait N, Gribble PL, Towhidkhal F, Ostry DJ.** Transfer and durability of acquired patterns of human arm stiffness. *Exp Brain Res* 170: 227–237, 2006.
- Darainy M, Towhidkhal F, Ostry DJ.** Control of hand impedance under static conditions and during reaching movements. *J Neurophysiol* 97: 2676–2685, 2007.
- Feldman AG.** Superposition of motor programs—I. Rhythmic forearm movements in man. *Neuroscience* 5: 81–90, 1980.
- Fisher NI.** *Statistical Analysis of Circular Data*. Cambridge, UK: Cambridge Univ. Press, 1993, p. 145–155.
- Fitts PM.** The information capacity of the human motor system in controlling the amplitude of movements. *J Exp Psychol* 47: 381–391, 1954.
- Franklin DW, Liaw G, Milner TE, Osu R, Burdet E, Kawato M.** Endpoint stiffness of the arm is directionally tuned to instability in the environment. *J Neurosci* 27: 7705–7716, 2007.
- Franklin DW, So U, Kawato M, Milner TE.** Impedance control balances stability with metabolically costly muscle activation. *J Neurophysiol* 92: 3097–3105, 2004.
- Gomi H, Kawato M.** Human arm stiffness and equilibrium-point trajectory during multi-joint arm movements. *Biol Cybern* 76: 163–171, 1997.
- Gomi H, Osu R.** Task dependent viscoelasticity of human multijoint arm and its spatial characteristic for interaction with environment. *J Neurosci* 18: 8965–8978, 1998.
- Gordon J, Gilford MH, Ghez C.** Accuracy of planar reaching movements. I. Independence of direction and extent variability. *Exp Brain Res* 99: 97–111, 1994.
- Gribble PL, Mullin LI, Cothros N, Mattar A.** Role of cocontraction in arm movement accuracy. *J Neurophysiol* 89: 2667–2677, 2002.
- Gribble PL, Ostry DJ.** Independent coactivation of shoulder and elbow muscles. *Exp Brain Res* 123: 355–360, 1998.
- Harris CM, Wolpert DM.** Signal-dependent noise determines motor planning. *Nature* 394: 780–784, 1998.
- Haruno M, Wolpert DM.** Optimal control of redundant muscles in step-tracking wrist movements. *J Neurophysiol* 94: 4244–4255, 2005.
- Hogan N.** The mechanics of multi-joint posture and movement control. *Biol Cybern* 52: 315–331, 1985.
- Mussa-Ivaldi FA, Hogan N, Bizzi E.** Neural, mechanical, and geometric factors subserving arm posture in humans. *J Neurosci* 5: 2732–2743, 1985.
- Osu R, Burdet E, Franklin DW, Milner TE, Kawato M.** Different mechanisms involved in the adaptation to stable and unstable dynamics. *J Neurophysiol* 90: 3255–3269, 2003.
- Osu R, Kamimura N, Iwasaki H, Nakano E, Harris CM, Wada Y, Kawato M.** Optimal impedance control for task achievement in the presence of signal dependent noise. *J Neurophysiol* 92: 1199–1215, 2003.
- Perreault EJ, Kirsch RF, Crago PE.** Voluntary control of static endpoint stiffness during force regulation tasks. *J Neurophysiol* 87: 2808–2816, 2002.
- Selen LP, Beek PL, van Dieen JH.** Impedance is modulated to meet accuracy demands during goal-directed arm movements. *Exp Brain Res* 172: 192–138, 2005.
- Shiller DM, Laboissiere R, Ostry DJ.** Relationship between jaw stiffness and kinematic variability in speech. *J Neurophysiol* 88: 2329–2340, 2002.
- Todorov E, Jordan MI.** Optimal feedback control as a theory of motor coordination. *Nat Neurosci* 5: 1226–1235, 2002.
- van Beers RJ, Haggard P, Wolpert DM.** The role of execution noise in movement variability. *J Neurophysiol* 91: 1050–1063, 2004.